The influence of Zn²⁺-binding motif sequence on the catalytic activity of transthyretin towards amyloid beta

Waralee Krainara, Ladda Leelawatwattana, Porntip Prapunpoj*

Department of Biochemistry, Division of Health and Applied Sciences, Faculty of Science, Prince of Songkla University, Songkhla 90110 Thailand

*Corresponding author, e-mail: porntip.p@psu.ac.th

ABSTRACT: The proteolysis property of transthyretin (TTR) was believed to be important for physiological processes and have therapeutic potential. In the present study, we interchanged the corresponding sequences of Zn²⁺ binding motif between human and *Crocodylus porosus* TTRs. The kinetic parameters of the proteolytic activity towards amyloid beta 1-42 (Aβ$_{1-42}$) of the mutated TTRs were determined by using a sensitive fluorescence-based method, and compared with the wild types. The results showed that *C. porosus* TTR with Zn²⁺-binding motif sequence of human TTR (hu-motif/crocTTR) has apparent K_m (K_m^{app}) of 118 ± 13 μM which was significantly higher than those for human TTR (53.6 ± 1.5 μM), *C. porosus* TTR (crocTTR) (30.2 ± 4.0 μM), and human TTR with Zn²⁺-binding motif sequence of *C. porosus* TTR (croc-motif/huTTR) (53.4 ± 0.87 μM). In addition, the catalytic efficiency (V_{max}/K_m^{app}) of croc-motif/huTTR (1.16 ± 0.0066 RFU min⁻¹μM⁻¹) was significantly higher than human TTR (0.639 ± 0.0085 RFU min⁻¹μM⁻¹) but similar to those of crocTTR (1.11 ± 0.082 M⁻¹min⁻¹) and hu-motif/crocTTR (0.894 ± 0.031 RFU min⁻¹μM⁻¹). The obtained results provided insight of the influence of the Zn²⁺-binding motif sequence and the evolutionary change structure on the proteolytic activity towards Aβ of TTR and useful information for designing a therapeutic TTR.

KEYWORDS: amyloid beta, *Crocodylus porosus*, proteolytic activity, transthyretin, zinc binding motif

INTRODUCTION

Transthyretin (TTR), a major thyroid hormones distributor in plasma and cerebrospinal fluid, is mainly synthesized in the liver and the choroid plexus of the brain [1]. Its native molecule comprises four identical subunits and has a molecular weight of 55 kDa [2]. The primary structure of TTR, particularly the thyroid hormone (TH) binding region, has been conserved through evolution [3, 4]. Predominant changes in TTR structure occur at the N-terminal sequence, and the N-terminal region of the avian and the reptilian are longer and more hydrophobic than that of the eutherian [5, 6]. The changes influence on not only the function of TTR as distributors for TH and retinal [7, 8], but also its catalytic property [9, 10]. Beside functioning as TH and retinal distributors, TTR proteolytic activity towards amyloid beta (Aβ) and a few specific target proteins is evidenced for its important physiological roles in the central and peripheral nervous systems of human [11, 12]. Amyloid beta 1-42 (Aβ protein fragment 1-42, Aβ$_{1-42}$) is a key pathophysiological hallmark of Alzheimer's disease; its detection in human plasma

has recently been possible using a dot blot sandwich immunoassay with the gold nanoparticles as signal label [13]. Based on the experimental evidence, TTR was identified as a metallopeptidase having 3 amino acid residues (His⁸⁸His⁹⁰Glu⁹²) in HXHXE motif as the specific binding site for the catalytic Zn²⁺ [14]. Since the motif is conserved only in human and some primate TTRs, the proteolytic activity of TTR was thus suggested as a recent evolutionary event [14].

As mention earlier, there are two major synthesis sites of TTR in mammalian, the liver and the choroid plexus of the brain. The synthesis of TTR in the choroid plexus first appeared at the stage of the stem-reptiles [15]. For a particular reptile like *Crocodylus porosus*, *TTR* gene is strongly expressed in the choroid plexus but not at all in the liver of the adults [7, 15, 16], indicating the predominant function of TTR in the animal brain. Interestingly, besides the function of human TTR as thyroid hormones and retinal distributors were evidenced in *Crocodylus porosus* TTR (crocTTR) [6, 15], its similar proteolytic activity towards Aβ was also elucidated [17]. Although the entire amino

acid sequence of crocTTR polypeptide is highly conserved and similar to that of the eutherian TTRs, the Zn^{2+}-chelating sequence HXHXE does not exist in the reptile TTR. The addition of a few amino acid residues to the N- and/or C-terminal sequence of *C. porosus* and human TTR polypeptides resulted in chimeric TTRs with higher and more specificity of the proteolytic activity [9]. Accordingly, we hypothesized not only Zn^{2+}-chelating motif sequence HXHXE but also the sequence nearby particularly those in the N- and C-terminal regions of TTR polypeptide play roles in the proteolytic activity of TTR. Herein, we synthesized two mutated TTRs by interchanging the corresponding sequences to Zn^{2+}-binding motif sequence between human TTR and crocTTR whose N-terminus has three additional amino acids; then, their catalytic activities towards $A\beta_{1-42}$ were determined and compared. Our results demonstrated the impact of the evolutionary changes in the structure on the efficiency of the catalytic activity of TTR.

MATERIALS AND METHODS

Reagents and chemicals

Oligonucleotide primers were synthesized by Operon (Eurofins MWG Operon, Huntsville, AL, USA). PCR and plasmid purification kits were from GibcoBRL (Long Island, NY, USA) and Qiagen (Hilden, Germany), and DNA ligase was from New England Biolabs (Ipswich, MA, USA). *Taq* DNA polymerase was a product of Invitrogen (Carlsbad, CA, USA). Horseradish peroxidase conjugated anti-rabbit IgG and the ECL kit were from Calbiochem (San Diego, CA, USA) and Amersham Bioscience (Chalfont St Giles, UK), respectively. Human RBP purified from urine was from RDI (Fitzgerald, MA, USA). Cibacron blue 3GA were products of Sigma (St Louis, MO, USA). Human $A\beta_{1-142}$ was from Millipore (KGaA, Darmstadt, Germany), Alexa Fluor 488 TFP ester from Molecular Probes (Life technologies, USA), and Bio-gel P2 from Bio-Rad (CA, USA). All of other chemicals used were of the analytical grade.

Purification of human TTR from plasma

TTR in human plasma was isolated using two purification steps. Briefly, human plasma was loaded onto a Cibacron blue 3GA column for removing the abundant plasma albumin. Then, the concentrated unbound fraction was further purified by preparative discontinuous native-PAGE (12% resolving and 4% stacking gels). The concentration and purity of the purified TTR were analyzed by the Bradford assay [18] and SDS-PAGE, respectively.

Construction, cloning, and expression of TTR cDNAs

The cDNAs coding for TTRs were mutated by interchanging of the Zn^{2+}-binding motif between human and *C. porosus* TTR (Fig. 1). The mutant TTRs comprised human TTR in which $His^{88}Glu^{89}His^{90}Ala^{91}Glu^{92}$ were replaced with $His^{88}Glu^{89}Tyr^{90}Ala^{91}Asp^{92}$ of *C. porosus* TTR (croc-motif/huTTR) and *C. porosus* TTR in which $His^{88}Glu^{89}Tyr^{90}Ala^{91}Asp^{92}$ were replaced with $His^{88}Glu^{89}His^{90}Ala^{91}Glu^{92}$ of human TTR (hu-motif/crocTTR). The two mutated TTR cDNAs containing *Xho*I at the 5′ end and *EcoR*I at the 3′ end for ligation into pPIC9 expression vector were prepared by six sequential PCR steps using human wild type TTR cDNA or *C. porosus* wild type TTR cDNA as template and primers as listed in Table 1. The mutated TTR sequences were confirmed by DNA sequencing prior to ligating to the expression vector. Then, the recombinant TTR vectors were introduced into *Pichia pastoris* strain GS115 by electroporation. The *Pichia* transformants with phenotype His^+Mut^+ (histidine synthesis and methanol utilization positive) were screened from His^+Mut^s (histidine synthesis and methanol utilization slow) by observation cell growth on minimal dextrose medium (MD) and minimal methanol medium (MM). His^+Mut^+ transformants were selected for recombinant protein synthesis.

Synthesis and purification of the recombinant TTRs

The recombinant proteins were produced in *P. pastoris* as described previously [8, 19]. In brief, the *Pichia* clone was induced to express the recombinant TTR with methanol in culture medium for 3 days. After the induction, the secreted recombinant TTR in culture medium was concentrated by ultrafiltration prior to purification by preparative discontinuous native-PAGE (12% resolving and 4% stacking gels). The purity and concentration of the recombinant TTRs were determined as described for human TTR.

Physicochemical analysis of the purified TTRs

The molecular mass of TTR subunits and the electrophoretic migration of TTR under native condition were analyzed by SDS-PAGE (12% resolving gel and 4% stacking gel) and native PAGE (10% resolving gel and 4% stacking gel), respectively. The protein

```
Human        GPT     GTGESKC ----- EEEFVEGIYK VEIDTKSYWK ALGISPF HEH AE VVFTANADS GPRRYTIAAL LSPYSYSTTA VVTNPKE

Crocodile    A*L  VSH  *SID*** ----- D*K******R **F**S**** ***L***Y *D********* *H*H****** ***F****** **SD*Q*
             1 3  4   10        70         80          90       100        110        120
```
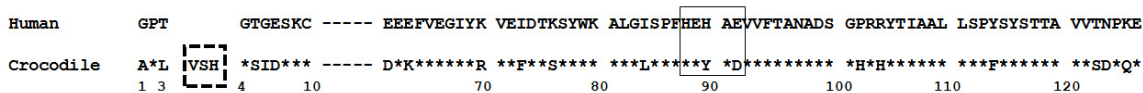
Fig. 1 Comparison of the amino acid sequence of human and *C. porosus* TTRs. The amino acid sequence of TTR from *C. porosus* was aligned with that of human TTR. Asterisk indicates the residues identical to those of human TTR and the numbering of residues is based on human TTR. The dot square frame at the N-terminal region corresponds to the additional three amino acids in *C. porosus* whereas the black square frame shows the difference of amino acids in the Zn^{2+}-binding site of human TTR compared to *C. porosus* TTR.

Table 1 Specific oligonucleotide primers used to generate cDNAs for croc-motif/huTTR and hu-motif/crocTTR. In order to prepare the cDNAs, PCR were carried out for 6 steps. The nucleotide sequence of the corresponding Zn^{2+}-binding motif sequence of *C. porosus* TTR in the primers is underlined, and that of human TTR is in bold.

TTR cDNA type	PCR step	Primer 5′ → 3′	
croc-motif/huTTR	1	CTCGAGAAAAGAGGCCCAACGGGC	Sense
		TCGTTGGCTGTGAATACCACATCTGCATACTCATGG	Antisense
	2	CTCGAGAAAAGAGGCCCAACGGGC	Sense
		TGTAGCGGCGGGGGCCGGAGTCGTTGGCTGTG	Antisense
	3	CTCGAGAAAAGAGGCCCAACGGGC	Sense
		TAGGGGCTCAGCAGGGCGGCAATGGTGTAGCGGC	Antisense
	4	CTCGAGAAAAGAGGCCCAACGGGC	Sense
		ACGACAGCCGTGGTGGAATAGGAGTAGGGGCTCAG	Antisense
	5	CTCGAGAAAAGAGGCCCAACGGGC	Sense
		TCATTCCTTGGGATTGTGACGGACAGCCG	Antisense
	6	CTCGAGAAAAGAGGCCCAACGGGC	Sense
		AGGAGTGAATTCTCATTCCTTGGGATTGG	Antisense
hu-motif/crocTTR	1	TCTCTCGAGAAAAGAGCCCCACTGGTTTCCC	Sense
		ACCGGAATCATTAGCAGTGAAAACCAC**CTCAGCATGTTC**	Antisense
	2	TCTCTCGAGAAAAGAGCCCCACTGGTTTCCC	Sense
		AGCAATGGTATAATGACGGTGACCGGAATCATTAGC	Antisense
	3	TCTCTCGAGAAAAGAGCCCCACTGGTTTCCC	Sense
		AGAGAAAGGACTTAAGAGAGCAGCAATGGTATAATG	Antisense
	4	TCTCTCGAGAAAAGAGCCCCACTGGTTTCCC	Sense
		AGGGCTGTGGTTGAATAAGAGAAAGGAC	Antisense
	5	TCTCTCGAGAAAAGAGCCCCACTGGTTTCCC	Sense
		TGGATCACTGACAACAGCAGTGGTTG	Antisense
	6	TCTCTCGAGAAAAGAGCCCCACTGGTTTCCC	Sense
		ACGGAATTCTTATTCTTGTGGATCACTG	Antisense

bands were visualized by Coomassie blue staining. The crossed-reactivity of the recombinant TTRs was determined by Western blotting as described previously [8]. After blocking, the membrane was incubated with sheep polyclonal antibody against serum human TTR (dilution 1:20000) or rabbit polyclonal antibody raised against *C. porosus* TTR (dilution 1:5000) as a primary antibody and horseradish peroxidase (HRP)-linked sheep IgG (dilution 1:20000) or HRP-conjugated anti-rabbit IgG (dilution 1:2500) as a secondary antibody.

Aβ labeling with Alexa Fluor 488 TFP ester

$A\beta_{1-42}$ was labeled with Alexa Fluor 488 TFP ester as described previously [17]. The purification of the Alexa Fluor 488-labeled $A\beta_{1-42}$ from free dye was performed by size exclusion chromatography on Bio-gel P2. The concentration and degree of labeling of the purified labeled $A\beta_{1-42}$ were respectively calculated from the values of absorbance at 280 nm and 494 nm, as described in the manufacturer's protocol. The labeled $A\beta_{1-42}$ was analyzed by 16% Tricine SDS-PAGE for purity determination. Then, the fluorescence of the Alexa-labeled $A\beta_{1-42}$ was detected under UV light, and the peptide bands were visualized by Coomassie staining. The fluorescence spectrum and fluorescence signal intensity of the labeled $A\beta_{1-42}$ were analyzed by a spectrofluorophotometer (Shimadzu RF-1501, Japan) and a microplate reader (Synergy HT, Bio-Tek Instruments VT, USA), respectively.

Analysis of Alexa labeled $A\beta_{1-42}$ cleavage by TTRs

TTR at 2.42 µM was incubated with 30 µM Alexa labeled $A\beta_{1-42}$ in 50 µM Tris HCl, pH 7.5 for 0 and 20 min at 37 °C. Then the reactions were diluted with non-reducing loading buffer, pH 8.8 followed

by analysis on 19% Tris-tricine PAGE. The fluorescence signal of uncleaved and cleaved Alexa labeled $A\beta_{1\text{-}42}$s were detected under UV light prior staining with silver nitrate.

Kinetic assay

The catalytic kinetic assay of TTRs by using Alexa Fluor 488-labeled $A\beta_{1\text{-}42}$ as a substrate was described previously [17]. Briefly, purified TTR (7.3 µM for human TTR and croc-motif/huTTR, and 7.0 µM for crocTTR and hu-motif/crocTTR) was incubated with labeled $A\beta_{1\text{-}42}$ at different concentrations (0–66 µM), and the fluorescence intensity of the cleaved substrate was measured continuously by the Synergy HT microplate reader (Bio-Tek Instruments VT, USA) with excitation and emission wavelengths at 485 ± 20 nm and 528 ± 20 nm, respectively. The initial velocity (V_0) of each substrate concentration was calculated by the slope of curve, which was plotted between the normalized florescence intensity and time. The V_0 for each reaction was expressed as relative fluorescence unit per minute (RFU/min). The apparent Michaelis constant (K_m^{app}) and maximum velocity (V_{max}) were derived from Michaelis-Menten plot using nonlinear regression prior to the catalytic efficiency (V_{max}/K_m^{app}) was determined. Mean and standard deviation (SD) for these kinetic values in each experiment were calculated in three replications.

Statistical analysis

The K_m^{app}, V_{max} and V_{max}/K_m^{app} are showed as a mean $\pm$ standard error (SE). The data were compared using one-way ANOVA, and a post-hoc test to compare the difference between groups. *p*-values of less than 0.05 ($p < 0.05$) were considered to be significant.

RESULTS

The synthesis and purification of recombinant croc-motif/huTTR and hu-motif/crocTTR

The cDNAs for croc-motif/huTTR and hu-motif/crocTTR were constructed by 6 steps of PCR. The PCR product with an expected size of ~400 bp (corresponding to 127 or 130 amino acids of human TTR or crocTTR plus compatible restriction end sequence) could be obtained prior to ligation into expression vector. Nucleotide sequencing confirmed that the nucleotide sequence would code for the desired amino acid residues.

Table 2 Kinetic parameters of human TTR, croc-motif/huTTR, crocTTR and hu-motif/crocTTR using Alexa labeled $A\beta_{1\text{-}42}$ as substrate. Data were represented as mean $\pm$ standard error (SE) of 3 replicates. The difference of kinetic parameters between each TTR was analyzed by ANOVA followed by Scheffe as post-hoc test.

Type of TTR	K_m^{app} (µM)	V_{max} (RFU/min)	V_{max}/K_m^{app} (RFU µM^{-1}min^{-1})
human TTR	53.6 ± 1.5^a	34.2 ± 0.5^{ab}	0.639 ± 0.008^a
croc-motif/huTTR	53.4 ± 0.9^a	61.7 ± 1.2^a	1.160 ± 0.007^b
crocTTR	30.2 ± 4.0^a	31.7 ± 2.4^b	1.110 ± 0.082^{bc}
hu-motif/crocTTR	118 ± 13^b	103 ± 8.0^c	0.894 ± 0.031^{abc}

a,b,c indicate significance differences at $p < 0.05$.

The recombinant mutated TTRs were produced in the heterologous expression system of *P. pastoris*. The TTR in the culture supernatant was purified by preparative native-PAGE. The single bands of TTRs on native-PAGE (Fig. 2A) and the two bands corresponding to monomeric and dimeric TTRs on SDS-PAGE (Fig. 2B) confirmed that the two recombinant TTRs were successfully purified. Cross reactivity to specific antibody of the mutated TTRs were also determined. The result indicated that croc-motif/huTTR and hu-motif/crocTTR could cross react with antibody raised against human TTR and recombinant crocTTR, respectively (Fig. 2B).

Alexa labeled $A\beta_{1\text{-}42}$ cleavage by TTRs

$A\beta_{1\text{-}42}$ was labeled with Alexa Fluor 488 in order to determine proteolytic activity of all TTRs. The peptide to dye ratio was 1:0.2, and monomeric form was the major $A\beta_{1\text{-}42}$ to be labeled. Tricine-PAGE analysis showed 2 bands of Alexa labeled $A\beta_{1\text{-}42}$, which corresponded to the masses of ~4900 Da and ~4400 Da, respectively. Upon cleavage by TTR for 20 min, the decreases in intensity of the two major bands and the smaller band, with the size of ~3900 Da, ~2000 Da and ~1700 Da, respectively, could be observed under UV. From the analysis, croc-motif/huTTR and hu-motif/crocTTR could cleave Alexa labeled $A\beta_{1\text{-}42}$ faster than their wild type TTRs (Fig. 3).

Catalytic kinetic of TTRs

Kinetics parameters of all TTRs were calculated from Michaelis-Menten plot (Fig. 4). K_m^{app} of hu-motif/crocTTR (118 ± 13 µM) was significantly higher than crocTTR (30.2 ± 4.0 µM), human TTR (53.6 ± 1.5 µM), and croc-motif/huTTR (53.4 ± 0.87 µM) (Table 2). The catalytic efficiency V_{max}/K_m^{app} of croc-motif/huTTR
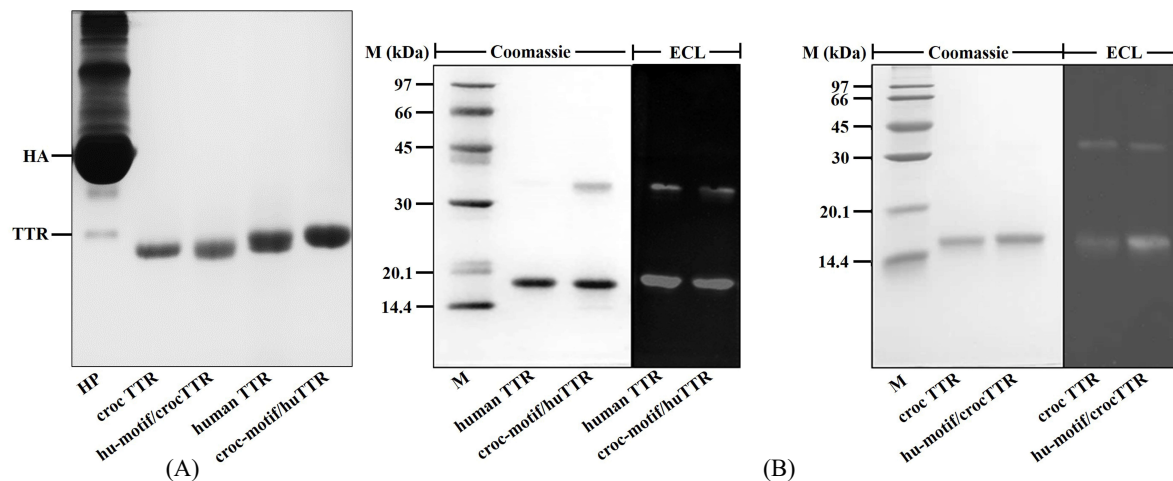
Fig. 2 Physiochemical characterization of TTRs. (A) The electrophoretic mobilities of TTRs under native condition were determined by native-PAGE (10% resolving and 4% stacking). Human plasma (HP) was loaded to show the position of TTR (TTR) and albumin (HA) in the plasma. (B) Subunit mass of croc-motif/huTTR and hu-motif/crocTTR were analyzed by SDS-PAGE (12% resolving and 4% stacking) and followed by Coomassie blue staining (Coomassie). Sizes of the TTR subunits were obtained by comparing their relative mobility with protein markers (M). Cross reactivities of croc-motif/huTTR and hu-motif/crocTTR to antibody raised against human TTR and crocTTR were determined by Western blot analysis prior to the detection of the signal with enhanced chemiluminescence (ECL).
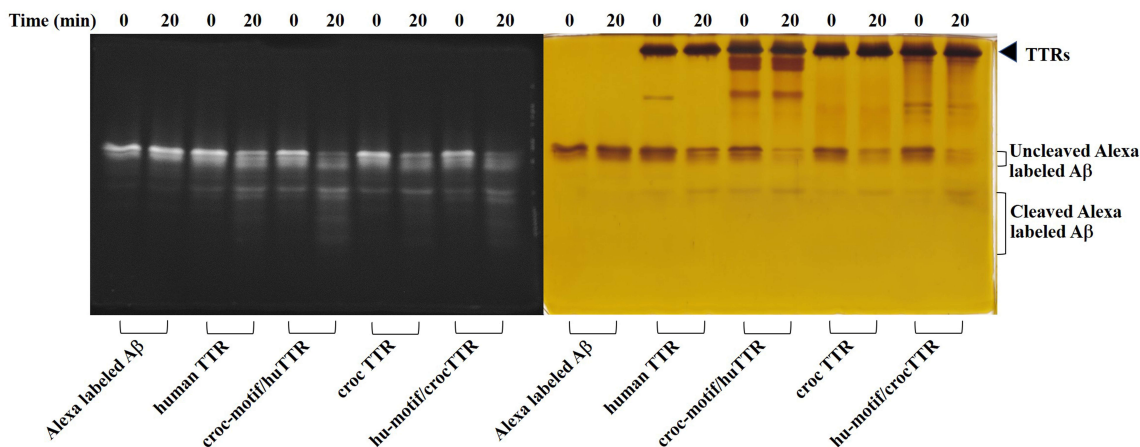

Fig. 3 Analysis of Alexa labeled $A\beta_{1-42}$ cleavage by TTRs. Aliquots (2.42 µM) of all studied TTRs were incubated with 30 µM of Alexa labeled $A\beta_{1-42}$. The reactions were then analyzed by 19% Tricine: PAGE followed by detection under UV (UV) and staining with silver nitrate (Silver).

(1.16 ± 0.0066 RFU $\text{min}^{-1}\mu\text{M}^{-1}$) was not different from crocTTR (1.11 ± 0.082 RFU $\text{min}^{-1}\mu\text{M}^{-1}$ and hu-motif/crocTTR (0.894 ± 0.031 RFU $\text{min}^{-1}\mu\text{M}^{-1}$) but significantly higher than human TTR (0.639 ± 0.0085 RFU $\text{min}^{-1}\mu\text{M}^{-1}$).

DISCUSSION

The proteolytic activity of TTR in human was reported in 2004 [11], and later its physiological substrates were identified, including amyloid β, amidated neuropeptide Y, and apolipoprotein A-I (apoAI) [20–22]. Subsequently, TTR was announced as a metallopeptidase with an inducible Zn^{2+}-binding site [14] in which His88, His90, and Glu92 serve as Zn^{2+}-complexing ligands [23]; in addition, the proteolytic activity of TTR has been proposed as a recent evolutionary event because the Zn^{2+}-binding motif HXHXE was conserved only in human and some non-human primates TTRs [14]. Our recent experiments showed that TTRs from
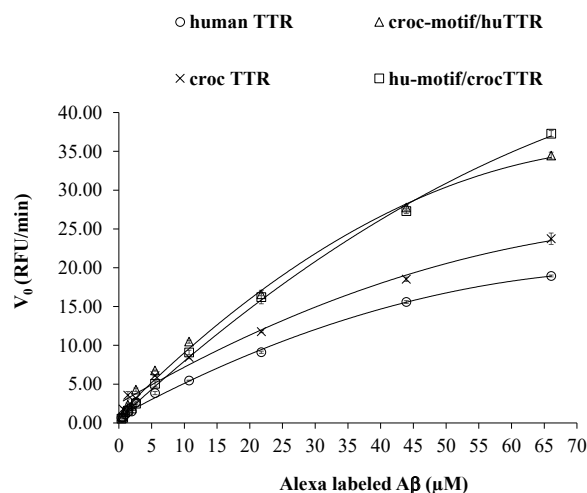
Fig. 4 Michaelis-Menten plot of the initial velocity of TTRs against Alexa labeled $A\beta_{1\text{-}42}$. The substrate concentrations used to perform the plot was 0.40–66 µM. Kinetic parameters including K_m^{app} and Vmax were calculated. Data were indicated as mean ± standard error (SE) of three replicates for each TTR.

Crocodylus porosus and *Gallus gallus* also have the proteolytic activity toward Aβ and other TTR substrates although the HXHXE motif does not exist [9, 17]. Moreover, changing N- and/or C- terminal region of TTR, to be longer and more hydrophobic, increases its proteolytic activity [9]. From these findings, it raised the hypothesis that the sequence nearby the catalytic site, especially those in the N- and C-terminus of TTR, participate in the proteolytic mechanism of TTRs. To elucidate, we synthesized mutated TTRs of *C. porosus* and human by interchanging the amino acids at the Zn^{2+}-binding motif HXHXE, and their proteolytic activities were compared with their relevant wild type TTRs.

Physicochemical properties of all TTRs were determined to confirm that their structures were similar to their native TTRs. Electrophoretic mobility of croc-motif/huTTR and hu-motif/crocTTR under native condition agreed well with other previous reported TTRs [24]. Both croc-motif/huTTR and hu-motif/crocTTR had subunit masses similarly to their wild type TTRs. Moreover, a minor band of dimeric TTR with the mass ∼2 folds of monomeric TTR was observed in both mutated TTRs, which also similar to their wild types. This result was in accordance with other TTRs previously reported [9, 19]. The dimer of TTR could be seen when TTR was not completely denatured even by heating under reducing condition for 30 min. This might be due to high strength of interaction between TTR dimer-dimer interfaces. Western blot result verified that bands appeared were TTRs because the proteins corresponding to monomer and dimer of TTR crossed react with specific antibodies. Taken as a whole, the physicochemical results suggested that TTRs used in the study have a proper quaternary structure which is necessary for their functions.

A sensitive fluorescence-based method for detecting the proteolytic activity towards Aβ and other substrates of TTR has been previously developed in our laboratory [10, 17]. The pattern and the kinetic parameters of the specific cleavage of $A\beta_{1\text{-}42}$ by *C. porosus* and human TTRs were also demonstrated [17]. By using Alexa Fluor 488 as a labeling dye, $A\beta_{1\text{-}42}$ was labeled as a monomeric form with intact conformation and functionality. Three possible positions of free primary amine group on $A\beta_{1\text{-}42}$ molecule that can be attached with Alexa fluor 488 include an amino group at the N-terminus and two amino groups of lysine residues at position 16 and 28. These three sites have similar potential to be labeled with Alexa Fluor 488 dye due to their similar pK_a values in the labeling reaction. The reported cleavage sites [12] together with the present results of $A\beta_{1\text{-}42}$ cleavage by TTRs (Fig. 3) which the cleaved fragment of ∼3900 Daltons (corresponding to ∼31 amino acids) was observed could suggest to high possibility of TTR to initially digest the peptide after Tyr10, and the predominant attachment of dye would possibly be at the side chain amino group of lysine position 16 of the peptide. Since tyrosine is an effective Alexa fluor 488 dye quencher [25], the cleavage of the labeled Aβ, therefore, results to lose the tyrosine quencher and the measurable fluorescence intensity of the peptide substrate. Fluorescence change within the linear range, which highly depended on the cleavage of Alexa Fluor 488 labelled $A\beta_{1\text{-}42}$ after Tyr10, was successfully used for calculation of an initial velocity of TTR towards $A\beta_{1\text{-}42}$ [17]. In this study, the linear changes of each studied reaction occurred within the first 5 min, and the values were subjected for determining the initial velocity and other kinetic parameters.

The kinetic parameter k_{cat}/K_m ratio is the specificity constant that has been used to measure the enzyme performance at steady state [26], and it reflects the overall ability in converting a substrate to product of an enzyme. The kinetic parameters including k_{cat}/K_m of the catalytic activity of human TTR and crocTTR were previous revealed by using $A\beta_{1\text{-}42}$ with Alexa fluor 488 labeling as substrate [17]. In comparison, crocTTR bound

$A\beta_{1-42}$ with higher strength than human TTR; in addition, the catalytic performance of the reptile TTR was also higher than the human TTR [17]. In this study, the kinetic parameters, particularly K_m^{app} and V_{max}/K_m^{app} values of the proteolytic activity of the two TTRs, were similar to previously reported results. This could imply to the consistent performance of the fluorescence-based method and the proper complex structure of the TTRs required for the study of their functions. Based on the kinetic parameters, it clearly indicated the direct influence of the Zn^{2+}-binding motif on K_m of the studied TTRs. However, the V_{max}/K_m^{app} value of croc-motif/huTTR increased almost double compared with human TTR, and the values of hu-motif/crocTTR and crocTTR were not significantly different. These could suggest an impact of the particular evolutionary change of the amino acid sequence locating nearby the Zn^{2+}-binding motif on the enzymatic performance of TTR. Moreover, the information obtained from our experimental results, based on its neuroprotective potential [27–29], may be helpful in designing TTR to be used as a therapeutic compound in the future.

CONCLUSION

We conducted the experiments with the objectives to determine whether the Zn^{2+} binding motif sequence detected in human TTR plays role in the proteolysis activity towards $A\beta$ of non-eutherian TTR and how the structural change of TTR during evolution impacts on the proteolysis activity, by interchanging the Zn^{2+} binding motif sequence of human TTR with the motif aligned sequence of *C. porosus* TTR. The obtained results suggest the influence of the motif sequence directly on the binding affinity between TTR and $A\beta$; whereas, the evolutionary change in the structure have impact on the efficiency of the catalytic activity of TTR.

REFERENCES

1. Makover A, Moriwaki H, Ramakrishnan R, Saraiva MJM, Blaner WS, Goodman DS (1988) Plasma transthyretin. Tissue sites of degradation and turnover in the rat. *J Biol Chem* **263**, 8598–8603.

2. Blake CCF, Geisow MJ, Oatley SJ, Rérat B, Rérat C (1978) Structure of prealbumin: secondary, tertiary and quaternary interactions determined by Fourier refinement at 1.8 Å. *J Mol Biol* **121**, 339–356.

3. Schreiber G, Prapunpoj P, Chang L, Richardson SJ, Aldred AR, Munro SL (1998) Evolution of thyroid hormone distribution. *Clin Exp Pharmacol Physiol* **25**, 728–732.

4. Schreiber G, Richardson SJ (1997) The evolution of gene expression, structure and function of transthyretin. *Comp Biochem Physiol* **116**, 137–160.

5. Richardson SJ (2007) Cell and molecular biology of transthyretin and thyroid hormones. *Inter Rev Cytology* **258**, 137–193.

6. Prapunpoj P, Leelawatwattana L (2009) Evolutionary changes to transthyretin: structure-function relationships. *FEBS J* **276**, 5330–5341.

7. Prapunpoj P, Richardson S, Schreiber G (2002) Crocodile transthyretin: structure, function, and evolution. *Am J Physiol Regul Integr Comp Physiol* **283**, R885–R896.

8. Leelawatwattana L, Praphanphoj V, Prapunpoj P (2011) Effect of the N-terminal sequence on the binding affinity of transthyretin for human retinol-binding protein. *FEBS J* **278**, 3337–3347.

9. Leelawatwattana L, Praphanphoj V, Prapunpoj P (2016) Proteolytic activity of *Crocodylus porosus* transthyretin protease and role of the terminal polypeptide sequences. *ScienceAsia* **42**, 190–200.

10. Tangthavewattana S, Leelawatwattana L, Prapunpoj P (2019) The hydrophobic C-terminal sequence of transthyretin affects its catalytic kinetics towards amidated neuropeptide Y. *FEBS Open Bio* **9**, 594–604.

11. Liz MA, Faro CJ, Saraiva MJ, Sousa MM (2004) Transthyretin, a new cryptic protease. *J Biol Chem* **279**, 21431–21438.

12. Costa R, Ferreira-da-Silva F, Saraiva MJ, Cardoso I (2008) Transthyretin protects against A-beta peptide toxicity by proteolytic cleavage of the peptide: a mechanism sentitive to the Kunitz protease inhibitor. *PLoS One* **3**, e2899.

13. Win SH, Wongchitrat P, Kladsomboon S, Dharmasaroja PA, Apiluk A (2019) Dot-blot sandwich immunoassay with silver signal enhancement for simple amyloid beta protein fragment 1-42 detection. *ScienceAsia* **45**, 260–267.

14. Liz MA, Leite SC, Juliano L, Saraiva MJ, Damas AM, Bur D, Sousa MM (2012) Transthyretin is a metallopeptidase with an inducible active site. *Biochem J* **443**, 769–778.

15. Richardson SJ (2009) Evolutionary changes to transthyretin: evolution of transthyretin biosynthesis. *FEBS J* **276**, 5342–5356.

16. Yamauchi K, Ishihara A (2009) Evolutionary changes to tranthyretin: developmentally regulated and tissue-specific gene expression. *FEBS J* **276**, 5357–5366.

17. Tola AJ, Leelawatwattana L, Prapunpoj P (2019) The catalytic kinetics of chicken transthyretin towards

human Aβ$_{1-42}$. *Comp Biochem Physiol C Toxicol Pharmacol* **226**, ID 108610.

18. Bradford MM (1976) A rapid and sensitive method for the quantitation of microgram quantities of protein utilizing the principle of protein-dye binding. *Anal Biochem* **72**, 248–254.

19. Prapunpoj P, Leelawatwatana L, Schreiber G, Richardson SJ (2006) Change in structure of the N-terminal region of transthyretin produces change in affinity of transthyretin to T4 and T3. *FEBS J* **273**, 4013–4023.

20. Costa R, Gonçalves A, Saraiva MJ, Cardoso I (2008) Transthyretin binding to A-beta peptide-Impact on A-beta fibrillogenesis and toxicity. *FEBS Lett* **582**, 936–942.

21. Liz MA, Gomes CM, Saraiva MJ, Sousa MM (2007) ApoA-I cleaved by transthyretin has reduced ability to promote cholesterol efflux and increased amyloidogenicity. *J Lipid Res* **48**, 2385–2395.

22. Liz MA, Fleming CE, Nunes AF, Almeida MR, Mar FM, Choe Y, Craik CS, Power JC, et al (2009) Substrate specificity of transthyretin: identification of natural substrates in the nervous system. *Biochem J* **419**, 467–474.

23. Gouvea IE, Kondo MY, Assis DM, Alves FM, Liz MA, Juliano MA, Juliano L (2013) Studies on the peptidase activity of transthyretin (TTR). *Biochimie* **95**, 215–223.

24. Richardson SJ, Bradley AJ, Duan W, Wettenhall RE, Harms PJ, Babon JJ, Southwell BR, Nicol S, et al (1994) Evolution of marsupial and other vertebrate thyroxine-binding plasma proteins. *Am J Physiol* **266**, R1359–R1370.

25. Chen H, Ahsan SS, Santiago-Berrios MB, Abruña HD, Webb WW (2010) Mechanisms of quenching of alexa fluorophores by natural amino acids. *J Am Chem Soc* **132**, 7244–7245.

26. Koshland DE (2002) The application and usefulness of the ratio kcat/KM. *Bioorganic Chem* **30**, 211–213.

27. Li X, Zhang X, Ladiwala ARA, Du D, Yadav JK, Tessier PM, Wright PE, Kelly JW, et al (2013) Mechanisms of transthyretin inhibition of β-amyloid aggregation *in vitro*. *J Neurosci* **33**, 19423–19433.

28. Yang DT, Joshi G, Cho PY, Johnson JA, Murphy RM (2013) Transthyretin as both a sensor and a scavenger of beta-amyloid oligomers. *Biochemistry* **52**, 2849–2861.

29. Silva CS, Eira J, Ribeiro CA, Oliveira A, Sousa MM, Cardoso I, Liz MA (2017) Transthyretin neuroprotection in Alzheimer's disease is dependent on proteolysis. *Neurobiol Aging* **59**, 10–14.